LASER INTERFEROMETER GRAVITATIONAL WAVE OBSERVATORY
- LIGO -
CALIFORNIA INSTITUTE OF TECHNOLOGY
MASSACHUSETTS INSTITUTE OF TECHNOLOGY

Technical Note **LIGO-T070236-00-D** 2020/09/07

Measuring The Hubble Constant With Dynamical Tides In Inspiraling Neutron Star Binaries

James Sunseri, Mentor: Hang Yu

Distribution of this document:

Detector Group

California Institute of Technology
LIGO Project, MS 100-36
Pasadena, CA 91125
Phone (626) 395-2129
Fax (626) 304-9834
E-mail: info@ligo.caltech.edu

Massachusetts Institute of Technology
LIGO Project, NW22-295
Cambridge, MA 02139
Phone (617) 253-4824
Fax (617) 253-7014
E-mail: info@ligo.mit.edu

LIGO Hanford Observatory
PO Box 159
Richland, WA 99352
Phone (509) 372-8106
Fax (509) 372-8137
E-mail: info@ligo.caltech.edu

LIGO Livingston Observatory
19100 LIGO Lane
Livingston, LA 70754
Phone (225) 686-3100
Fax (225) 686-7189
E-mail: info@ligo.caltech.edu

http://www.ligo.caltech.edu/

Abstract

The "Hubble Tension" is a large, newfangled problem in astronomy which has even larger cosmological consequences in its eventual resolve. Currently all calibration methods of the constant rely on the use of the electromagnetic spectrum-a method that does not rely on EM light but instead solely on gravitational radiation could prove extremely useful as both a backup for the unreliability of multi-messenger astronomy at its current state and as a new lens into cosmology which could potentially expand our understanding of light, gravity, and the universe. To extract a cosmological redshift from a gravitational waveform, one can look at both the point particle approximation phase contribution and the tidal phase contribution to the total phase of a gravitational waveform which allows for a break in the redshift degeneracy found in the mass parameters, which we can exploit to extract a cosmological redshift and thus the Hubble constant. Our analysis incorporates both f-modes and r-modes into the tidal phase contribution that are found in binary neutron star inspirals. We use the Fisher Matrix Analysis to generate our relevant possible errors on each parameter of the waveform.

1 Introduction

The Hubble-Lemaitre Constant H_0 is an important quantity in cosmology because it characterizes the rate at which the Universe is expanding, and it can be measured from a cosmological distance-redshift relation. However, two classical methods of measuring H_0 have led to seemingly inconsistent results, known as the "Hubble tension". One method uses type Ia supernovae (whose redshifts are provided by their spectra) as "standard candles" to infer the (luminosity) distance [1], while the other method relies on the acoustic features in the Cosmic Microwave Background (whose redshift corresponds to the surface of last scattering and is well-calculated) as a "standard ruler" to measure the (angular-diameter) distance [2]. The tension has triggered people's interests in searching for alternative methods of constraining H_0, and it turns out that gravitational-wave (GW) observations is a promising candidate.

It has been well realized that a GW signal can serve as a "standard siren", as one can easily obtain the source's luminosity distance from the signal's amplitude. If one can also somehow infer the source's redshift, it will then allow for a measurement H_0. One way to achieve so is to identify the host galaxy with an EM counterpart, and this method has been successfully demonstrated by the GW170817 event [3]. However, it may not be guaranteed that an EM counterpart can always be found (e.g., the line of sight to the source may lie in the Galactic plane). Thus a way of inferring the redshift using the GW signal alone would be of great significance. One such possibility is to use the internal modes of a neutron star. Under certain conditions the neutron stars cause tidal effects on each other which excite modes within the neutron stars. The following technique was used by [4], except they only considered the effects of the specific f and g modes, our analysis will focus primarily on the r-mode as well as inertial modes in general within the neutron stars. We will choose to focus primarily on the r-mode because it is now thought to have a considerably strong supplemental effect on the merger for the possible detectable frequency range of future generation detectors. For a given binary neutron star inspiraling gravitational wave data we are able to measure the r-mode resonance which allows us to find the redshifted spin frequency of the binary. This spin frequency can be mapped to the spin parameter referred to as $\chi = S/M^2$, where $S \sim f_{spin} M R^2$ is referring to the spin angular momentum. The mass is redshifted by a factor of $(1 + z)$. This measured value of χ is really shifted by a factor of $1/(1 + z)^2$. With this redshifted spin parameter we can compare it to the Point Particle Orbit which also gives us a measurement of χ, this measurement of the spin parameter experiences no redshift. By comparing the two measurements of χ we are able to deduce what the redshift value z would be for a given binary. We will finally use the Fisher Matrix technique to determine how well we can measure the cosmological redshift z.

2 Theory

In this section we will discuss the most important background theory to better understand the methodology. As two neutron stars begin to inspiral gravitational waves are emitted that traverse across spacetime to get to us. As those waves make their way to us the frequency is undergoing a redshift in the form $f \to f/(1 + z)$ while the detectable phase shift of the waveform remains unaffected. Since the phase is dependent on the frequency of the waveform, there needs to be an inverse redshift effect to combat this. As discussed in [4] this can be done with f-modes because the point particle phase contribution is a Post-Newtonian effect which implies that the mass must undergo the transformation $M \to M(1 + z)$ to preserve phase shift, but for the tidal phase shift contribution this does not occur since it is a direct result of interior neutron star physics. This breaks a degeneracy between mass and redshift which allows for a measurement of the redshift simultaneous to a measurement of the luminosity distance if the equation of state of a neutron star is known.

We use a similar concept except for a couple key differences. Instead of f-modes we turn to r-modes and other inertial modes because they are capable of achieving resonance within the LIGO/VIRGO frequency band. These new inertial modes are a bi product of the effects of spin and tidal forces on the interior of the neutron star. Now we look to the spin parameter χ mentioned earlier to extract a redshift. We know from Binary Black Hole observations that χ should remain unredshifted for the point particle phase contribution while χ does become redshifted by $\chi \to \chi/(1+z)^2$ for the tidal phase contribution. χ is redshifted in this way because $\chi \sim \Omega/M$ and we see that $M \to M(1 + z)$ as well as $\Omega \to \Omega/(1 + z)$ which combines to yield the total redshift factor on χ above.

In this analysis we write in Geometric Units where [G = c = 1] for simplicity.

2.1 Gravitational Waveform

As discussed in [5], a waveform for gravitational waves is denoted as $h(t)$ but we operate in the frequency domain by performing a fourier transform

$$\tilde{h}(f) \equiv \int_{-\infty}^{\infty} e^{2\pi i f t} h(t) dt \tag{1}$$

which yields a more useful version of the waveform

$$\tilde{h}(f) = \frac{Q}{D_L}\mathcal{M}^{5/6} f^{-7/6} \exp\left(i\Phi(f)\right) \tag{2}$$

for $f \geq 0$. Where D_L denotes the luminosity distance to the binary, $\mathcal{M}$ denotes the chirp mass, and Q is the detector sensitivity which we take to be ~ 1 for this project. The phase consists of two major contributing factors: the point particle orbit approximation and the tidal modes effects denoted as $\phi_{pp}(f)$ and $\phi_{tidal}(f)$. This waveform in total consists of 10 parameters $(\theta) = (D_L, \mathcal{M}, \mu, t_c, \phi_c, \psi_1, \psi_2, \Omega_1, \Omega_2, z)$ Those parameters are labeled the Luminosity Distance, Chirp Mass, Reduced Mass, Time of Coalescence, Phase of Coalescence, Inclination Angles of each star, Spin Frequency of each star, and Redshift of the Binary. The key here is to notice that we can measure a luminosity distance relatively easily from the amplitude of the waveform, and using information from the phase shift we can measure a redshift simultaneously.

2.2 Point Particle Phase Contribution

For our purposes we used the 1.5 order post-Newtonian point-particle frequency domain phase from [5] which also includes the effects of spin

$$\begin{aligned}\phi_{pp}(f) = 2\pi f t_c - \phi_c - \frac{\pi}{4} + \frac{3}{4}(8\pi\mathcal{M}f)^{-5/3} \\ \times\left[1 + \frac{20}{9}\left(\frac{743}{336} + \frac{11\mu}{4M}\right)x + (4\beta - 16\pi)x^{3/2}\right]\end{aligned} \tag{3}$$

The quantity β is essentially the spin parameter discussed earlier. We also define $x \equiv (\pi M f)^{2/3}$ and μ is the binary's reduced mass. Beta can be defined as the following

$$\beta \equiv M^{-2}\hat{L}\cdot\left[\left(\frac{113}{12} + \frac{25}{4}\frac{M_2}{M_1}\right)\vec{S_1} + \left(\frac{113}{12} + \frac{25}{4}\frac{M_1}{M_2}\right)\vec{S_2}\right] \tag{4}$$

and since we know that $\hat{L}\cdot\hat{S} = \cos\psi$, we can rewrite beta in terms of our input parameters

$$\begin{aligned}\beta = M^{-2}\left[\left(\frac{113}{12} + \frac{25}{4}\frac{M_2}{M_1}\right)(I_1\cdot\Omega_1\cos\psi_1) + \right. \\ \left.\left(\frac{113}{12} + \frac{25}{4}\frac{M_1}{M_2}\right)(I_2\cdot\Omega_2\cos\psi_2)\right]\end{aligned} \tag{5}$$

Note that I is simply the moment of inertia, which can be calculated analytically as a function of mass for a polytropic model of k = 1.

2.3 Tidal Phase Contribution

For this project we focus on the 4 inertial modes discussed in [6]. In this paper the neutron star equation of state is approximated by a $k = 1$ polytropic model, the density is described by the following

$$\rho = C\left[\frac{\sin(\pi r/R)}{(\pi r/R)}\right]^k \tag{6}$$

This approximation allows us to use the results from Poisson for the orbital phase shift due to dynamical tidal resonance with the gravitomagnetic potential. Using the polytropic model captures the assumption made my most EOS models that radius and mass are nearly independent of eachother. As long as we assume a known EOS it will not introduce any further uncertainties to our problem.

$$(\Delta\Phi)_n^m = \frac{25\pi^2}{2304}\frac{(\mathfrak{p}_n^m)^2}{\hat{N}_n^m}\frac{(m-w_n^m)^2}{|w_n^m|^{4/3}}(a_\pm^m)^2\frac{R^4\Omega^{2/3}}{(M_1)^2(M_2)(M)^{1/3}} \tag{7}$$

Where $\hat{N}_n^m, \mathfrak{p}_n^m, w_n^m$ are all constants defined in Table II of [6] for k = 1. $a_\pm^m$ is one of the various dependencies on the parameter ψ (inclination angle)

$$\begin{aligned} a_\pm^2 &= \mp\sin\psi(\cos\psi \pm 1) \\ a_\pm^1 &= \pm(\cos\psi \pm 1)(2\cos\psi \mp 1) \\ a_\pm^1 &= \mp\sin\psi\cos\psi \end{aligned} \tag{8}$$

According to Poisson, "inertial modes of a rotating star are labelled by two integers: the first is m, which determines the $e^{im\phi}$ dependence of the velocity perturbation on the azimuthal angle ϕ [and] the second integer is n, which sequences the infinity of overtones for each value of m. Each inertial mode comes with a distinct eigenfrequency $\omega_n^m = w_n^m\Omega$, where Ω is the star's rotational angular velocity, and w_n^m is a number of order unity"

Whether or not we choose a_+^m or a_-^m depends on which mode is resonantly excited. This is determined by the tidal driving which should be decomposed into two terms oscillating at: $+im\Omega_{orb}t$ and $-im\Omega_{orb}t$. We observe that of the 4 distinct modes we examine in our work, the modes corresponding to $(m = 2,\ n = \bullet)$, $(m = 1,\ n = \mathrm{I})$, $(m = 0,\ n = \mathrm{I})$ all have positive eigenfrequencies and they are resonantly excited by the $e^{i\Phi}$ term in the equation below implying that a_+^m should be used for those modes. For the fourth distinct mode corresponding to $(m = 1,\ n = \mathrm{II})$ we find that it has a negative eigenfrequency and thus is excited by the $e^{-i\Phi}$ term in the equation below which implies that a_-^m should be used instead. For the tidal driving expression from [6] we have:

$$\mathcal{S} = \sum_{m\geq 0}\sum_n \mathcal{S}_n^m \tag{9}$$

$$\mathcal{S}_n^m \propto [a_+^m \mathrm{Re}(ie^{i\Phi}) + a_-^m \mathrm{Re}(ie^{-i\Phi})] \tag{10}$$

This accounts for four separate inertial modes acting on each star. These trigonometric dependencies that each mode has on the star's inclination angle allows us to be able to break a degeneracy between the inclination angle and redshift. This was a problem we were facing with only incorporating a single r-mode contribution as discussed in [7]. Below is a superposition of all inertial modes and their contribution to a total $\Delta\phi_{tidal}$. Each vertical green line is a resonance being achieved by the first neutron star and each vertical blue line is a resonance being achieved by the second neutron star, there are 8 total because each star has 4 distinct resonances being achieved by the 4 inertial modes.

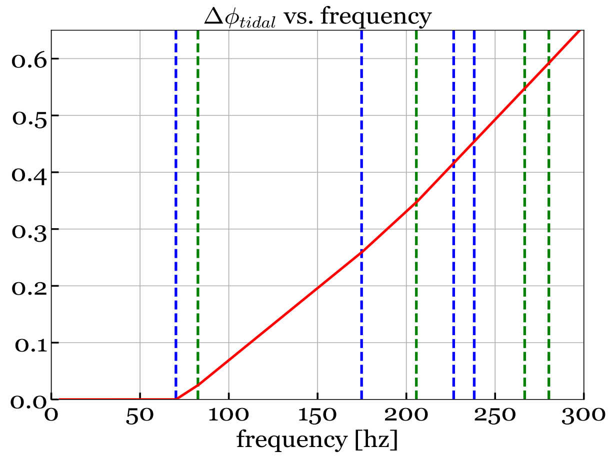

Figure 1: Inertial Mode Resonances at distinct resonant frequencies

2.4 Total Phase Contribution

Once we have successfully calculated the phase shifts for each of the 4 modes for both neutron stars we can use Eq. (32) of [8] to combine all the phase contributions:

$$\Phi_{total}(f) = \Phi_{pp}(f) - 2\sum_k \left(1 - \frac{f}{f_k}\right) \delta\phi_k \Theta(f - f_k) \tag{11}$$

Where we sum over all the modes for both stars, $\delta\phi_k$ is the phase shift due to the tidal resonance, f_k is the eigenfrequency corresponding to the kth mode and can be rewritten as $f_k = |w_n^m|\Omega/\pi$, and $\Theta(f - f_k)$ is the Heaviside step function. In doing this we are able to construct the total phase shift of the gravitational waveform.Lastly, we need to cut off the waveform at $2f_{isco}$ because the waveform is invalid for frequencies above this. So in total we end up with:

$$\tilde{h}(f) = \frac{Q}{D_L}\mathcal{M}^{5/6} f^{-7/6} \exp\left(i\Phi_{total}(f)\right)\Theta(2f_{isco} - f) \tag{12}$$

3 Method

3.1 Fisher Matrix Technique

In order to extract information about the relevant errors on a gravitational waveform's parameters, we need to utilize the Fisher Matrix Technique discussed in [5] where the Fisher Information Matrix is defined as

$$\Gamma_{ij} \equiv \left(\frac{\partial h}{\partial \theta^i}\middle|\frac{\partial h}{\partial \theta^j}\right) \tag{13}$$

The Fisher Information Matrix is constructed from an inner product between each partial derivative with respect to a given parameter. This inner product is defined as

$$(h_1|h_2) = 2\int_0^\infty \frac{\tilde{h}_1^*(f)\tilde{h}_2(f) + \tilde{h}_1(f)\tilde{h}_2^*(f)}{S_n(f)}df \tag{14}$$

Which we can then invert to get $\Sigma \equiv \Gamma^{-1}$ so we can extract the root-mean-square error in a given parameter θ^i

$$\sqrt{((\Delta\theta^i)^2)} = \sqrt{\Sigma^{ii}} \tag{15}$$

Once the error has been extracted we can know just how precisely each of the given parameters can be measured. By inverting the fisher matrix, we are creating a new covariance matrix to predict the covariances one will achieve after conducting an experiment. One can think of the diagonals of the information matrix as containing information about the possible precision on the error for each parameter, while the remaining entries contain information which explains how the errors for each parameter are related to each other.

3.2 Parameter Space Investigation

In order to ensure that our results were not tampered by numerical instabilities in the construction of the Fisher Information Matrix, we plotted the error of each parameter as a function of their step size used for numerical differentiation. We would then choose our step size for each numerical derivative based on the stable regions within these graphs. Below is an example of what this looked like.

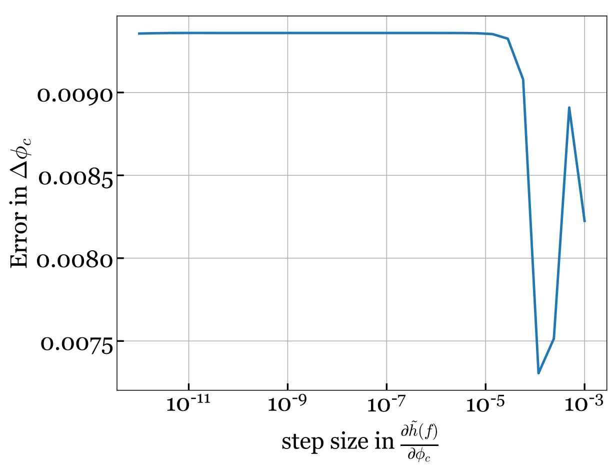

Figure 2: Error of ϕ_c with respect to step size

To choose a step size in a non stable region would create great problems in our predictions. Each graph looks different considering each parameter has a different role in the waveform, which means we can't simply pick one step size to work with for all parameters.

In order to examine degeneracies between parameters we constructed probability contours from the fisher information matrix. Below is probability contours between the error in redshift and one of the inclination angles before and after we incorporated several inertial modes. This shows an improvement in the degeneracy between the redshift and inclination angle from including the 4 inertial modes discussed in [6] as opposed to a single r-mode discussed in [7]

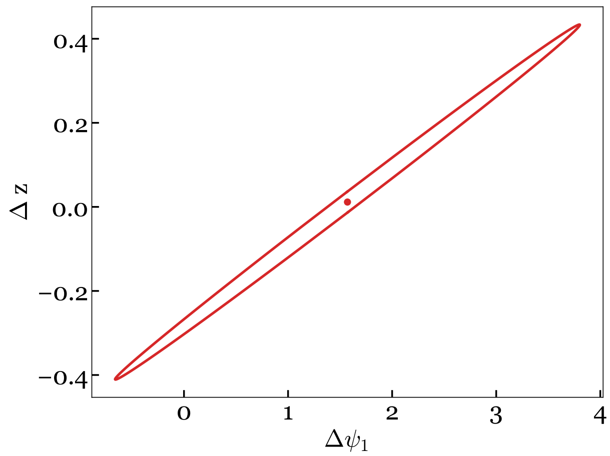

Figure 3: Error of z with respect to the error in ψ_1 using a single r-mode

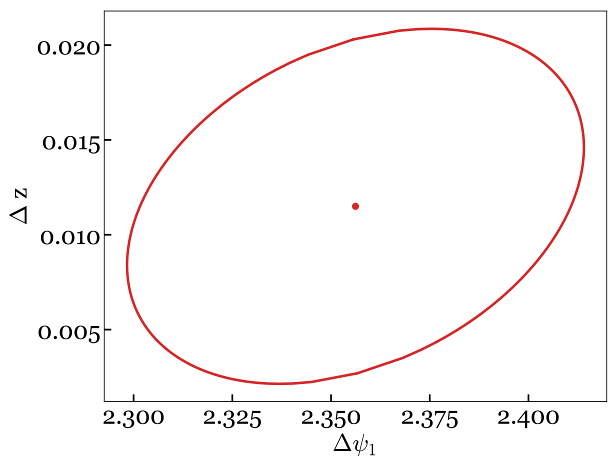

Figure 4: Error of z with respect to the error in ψ_1 using several inertial modes

4 Results

The relevant error we are concerned about in this analysis is with respect to a cosmological redshift z because inevitably it is what we need to properly calibrate the Hubble Constant. What we found in using a Cosmic Explorer Sensitivity Profile [9] was that for a realistic and probable set of parameters we can get a relative order $\Delta z/z \sim 4$ which is undesirable, but if we keep those inclination angles the same but increase the spin frequencies of the neutron stars to idealistic values we can cut that in half. We also found that if we use a realistic set of spin frequencies but utilize inclination angles that are idealistic we get a similar effect and can achieve $\Delta z/z \sim 2$ for low redshifts. If we use an optimistic set of parameters we can get a relative error less than order unity which can be beneficial.

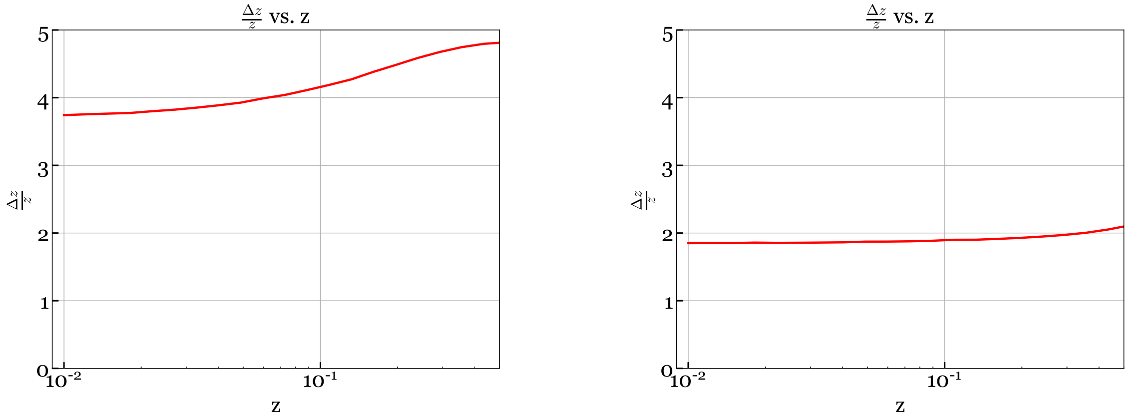

(a) $\psi_1, \psi_2 = \frac{\pi}{3}, \frac{\pi}{6}$
$\Omega_1, \Omega_2 = 30 \cdot 2\pi[\text{Hz}], 50 \cdot 2\pi[\text{Hz}]$

(b) $\psi_1, \psi_2 = \frac{\pi}{3}, \frac{\pi}{6}$
$\Omega_1, \Omega_2 = 100 \cdot 2\pi[\text{Hz}], 80 \cdot 2\pi[\text{Hz}]$

Figure 5: Relative Error of z with respect to z for most probable and realistic inclination angles.

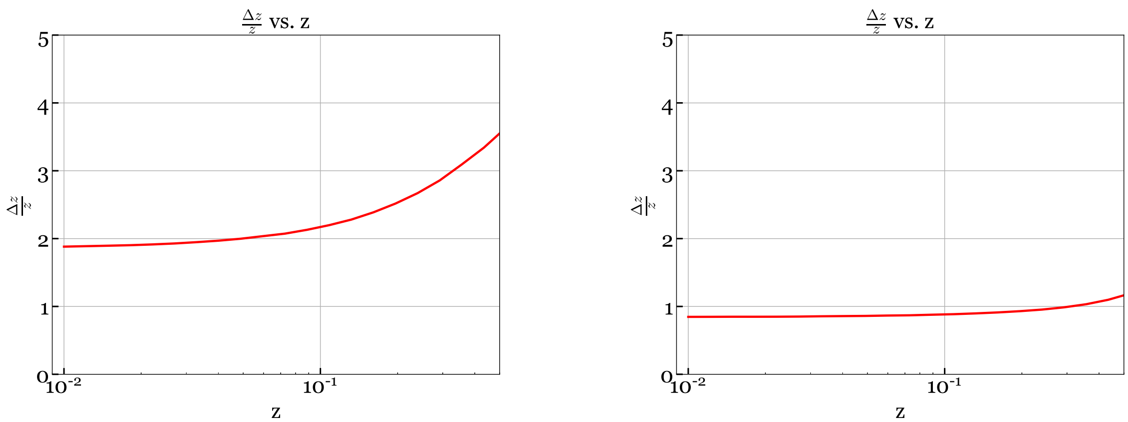

(a) $\psi_1, \psi_2 = \frac{3\pi}{4}, \frac{5\pi}{6}$
$\Omega_1, \Omega_2 = 30 \cdot 2\pi[\text{Hz}], 50 \cdot 2\pi[\text{Hz}]$

(b) $\psi_1, \psi_2 = \frac{3\pi}{4}, \frac{5\pi}{6}$
$\Omega_1, \Omega_2 = 100 \cdot 2\pi[\text{Hz}], 80 \cdot 2\pi[\text{Hz}]$

Figure 6: Relative Error of z with respect to z for most idealistic inclination angles

5 Conclusion

Using tidal effects in BNS mergers is crucial in our ability to measure redshifts simultaneously with luminosity distance for such events. While our analysis involving solely inertial modes discussed in [6] was not as precise as [4] and their use of f-modes, it is still valuable to have investigated this approach because we were able to successfully extract information about a redshift by exploiting the degeneracy between the spin parameter and the redshift in the point particle orbit approximation phase contribution and the tidal phase contribution. Looking forward to possible extensions of this research, it would be valuable to examine how well we could constrain the redshift of a binary where we combine both the effects of the inertial modes and the f-mode. Together we would likely be able to measure the redshift more precisely than [4] proposed. Furthermore, we would like to investigate how much more relaxed our assumptions can become about the equation of state of the neutron star.

References

[1] Adam G. Riess, Stefano Casertano, Wenlong Yuan, Lucas Macri, Beatrice Bucciarelli, Mario G. Lattanzi, John W. MacKenty, J. Bradley Bowers, WeiKang Zheng, Alexei V. Filippenko, and et al. Milky way cepheid standards for measuring cosmic distances and application to gaia dr2: Implications for the hubble constant. *The Astrophysical Journal*, 861(2):126, Jul 2018.

[2] Planck Collaboration, N. Aghanim, Y. Akrami, M. Ashdown, J. Aumont, C. Baccigalupi, M. Ballardini, A. J. Banday, R. B. Barreiro, N. Bartolo, S. Basak, R. Battye, K. Benabed, J. P. Bernard, M. Bersanelli, P. Bielewicz, J. J. Bock, J. R. Bond, J. Borrill, F. R. Bouchet, F. Boulanger, M. Bucher, C. Burigana, R. C. Butler, E. Calabrese, J. F. Cardoso, J. Carron, A. Challinor, H. C. Chiang, J. Chluba, L. P. L. Colombo, C. Combet, D. Contreras, B. P. Crill, F. Cuttaia, P. de Bernardis, G. de Zotti, J. Delabrouille, J. M. Delouis, E. Di Valentino, J. M. Diego, O. Doré, M. Douspis, A. Ducout, X. Dupac, S. Dusini, G. Efstathiou, F. Elsner, T. A. Enßlin, H. K. Eriksen, Y. Fantaye, M. Farhang, J. Fergusson, R. Fernandez-Cobos, F. Finelli, F. Forastieri, M. Frailis, A. A. Fraisse, E. Franceschi, A. Frolov, S. Galeotta, S. Galli, K. Ganga, R. T. Génova-Santos, M. Gerbino, T. Ghosh, J. González-Nuevo, K. M. Górski, S. Gratton, A. Gruppuso, J. E. Gudmundsson, J. Hamann, W. Handley, F. K. Hansen, D. Herranz, S. R. Hildebrandt, E. Hivon, Z. Huang, A. H. Jaffe, W. C. Jones, A. Karakci, E. Keihänen, R. Keskitalo, K. Kiiveri, J. Kim, T. S. Kisner, L. Knox, N. Krachmalnicoff, M. Kunz, H. Kurki-Suonio, G. Lagache, J. M. Lamarre, A. Lasenby, M. Lattanzi, C. R. Lawrence, M. Le Jeune, P. Lemos, J. Lesgourgues, F. Levrier, A. Lewis, M. Liguori, P. B. Lilje, M. Lilley, V. Lindholm, M. López-Caniego, P. M. Lubin, Y. Z. Ma, J. F. Macías-Pérez, G. Maggio, D. Maino, N. Mandolesi, A. Mangilli, A. Marcos-Caballero, M. Maris, P. G. Martin, M. Martinelli, E. Martínez-González, S. Matarrese, N. Mauri, J. D. McEwen, P. R. Meinhold, A. Melchiorri, A. Mennella, M. Migliaccio, M. Millea, S. Mitra, M. A. Miville-Deschênes, D. Molinari, L. Montier, G. Morgante, A. Moss, P. Natoli, H. U. Nørgaard-Nielsen, L. Pagano, D. Paoletti, B. Partridge, G. Patanchon, H. V. Peiris, F. Perrotta, V. Pettorino, F. Piacentini, L. Polastri, G. Polenta, J. L. Puget, J. P. Rachen, M. Reinecke, M. Remazeilles, A. Renzi, G. Rocha, C. Rosset, G. Roudier, J. A. Rubiño-Martín, B. Ruiz-Granados, L. Salvati, M. Sandri, M. Savelainen, D. Scott, E. P. S. Shellard, C. Sirignano, G. Sirri, L. D. Spencer, R. Sunyaev, A. S. Suur-Uski, J. A. Tauber, D. Tavagnacco, M. Tenti, L. Toffolatti, M. Tomasi, T. Trombetti, L. Valenziano, J. Valiviita, B. Van Tent, L. Vibert, P. Vielva, F. Villa, N. Vittorio, B. D. Wandelt, I. K. Wehus, M. White, S. D. M. White, A. Zacchei, and A. Zonca. Planck 2018 results. vi. cosmological parameters, 2018.

[3] B. P. Abbott and et al. A gravitational-wave standard siren measurement of the Hubble constant. *Nature*, 551(7678):85–88, November 2017.

[4] Chris Messenger and Jocelyn Read. Measuring a cosmological distance-redshift relationship using only gravitational wave observations of binary neutron star coalescences. *Physical review letters*, 108(9):091101, 2012.

[5] Curt Cutler and Eanna E Flanagan. Gravitational waves from merging compact binaries: How accurately can one extract the binary's parameters from the inspiral waveform? *Physical Review D*, 49(6):2658, 1994.

[6] Eric Poisson. Gravitomagnetic tidal resonance in neutron-star binary inspirals. *Physical Review D*, 101(10):104028, 2020.

[7] Eanna E Flanagan and Etienne Racine. Gravitomagnetic resonant excitation of rossby modes in coalescing neutron star binaries. *Physical Review D*, 75(4):044001, 2007.

[8] Hang Yu and Nevin N. Weinberg. Dynamical tides in coalescing superfluid neutron star binaries with hyperon cores and their detectability with third-generation gravitational-wave detectors. *Monthly Notices of the Royal Astronomical Society*, 470(1):350–360, May 2017.

[9] David Reitze, Rana X Adhikari, Stefan Ballmer, Barry Barish, Lisa Barsotti, GariLynn Billingsley, Duncan A. Brown, Yanbei Chen, Dennis Coyne, Robert Eisenstein, Matthew Evans, Peter Fritschel, Evan D. Hall, Albert Lazzarini, Geoffrey Lovelace, Jocelyn Read, B. S. Sathyaprakash, David Shoemaker, Joshua Smith, Calum Torrie, Salvatore Vitale, Rainer Weiss, Christopher Wipf, and Michael Zucker. Cosmic explorer: The u.s. contribution to gravitational-wave astronomy beyond ligo, 2019.